

Evidence for ferromagnetism in KTaO_3 heterointerface superconductors

Zhongfeng Ning,¹ Jiahui Qian,¹ Yixin Liu,^{2,3} Fan Chen,^{2,3} Guanqun Zhang,¹ Gang Mu,^{2,3,*} and Wei Li^{1,4,*}

¹*State Key Laboratory of Surface Physics and Department of Physics, Fudan University, Shanghai 200433, China*

²*State Key Laboratory of Functional Materials for Informatics,
Shanghai Institute of Microsystem and Information Technology,
and Center for Excellence in Superconducting Electronics,
Chinese Academy of Sciences, Shanghai 200050, China*

³*University of Chinese Academy of Sciences, Beijing 100049, China*

⁴*Collaborative Innovation Center of Advanced Microstructures, Nanjing University, Jiangsu 210093, China*

(Dated: February 6, 2023)

The coexistence of superconductivity and ferromagnetism has been a long-standing issue in the realm of unconventional superconductivity due to the antagonistic nature of these two ordered states. Experimentally identifying and characterizing new fascinating heterointerface superconductors that coexist with magnetism are challenging. Here, we report the experimental observation of long-range ferromagnetic order at the verge of two-dimensional superconductivity at the KTaO_3 heterointerfaces. Remarkably, the fingerprint of ferromagnetism is the existence of in-plane magnetization hysteresis loop persisting up to room temperature observed in direct current superconducting quantum interference device measurements. Furthermore, first-principles calculations suggest that the robust ferromagnetism is attributed to the presence of oxygen vacancies that localize electrons in nearby Ta $5d$ states. Our findings not only unveil the KTaO_3 heterointerfaces to be unconventional superconductors with time-reversal symmetry breaking, but also inject a new momentum to the study of a delicate interplay of superconductivity and magnetism boosted by the strong spin-orbit coupling inherent to the heavy Ta in $5d$ orbitals of KTaO_3 heterointerfaces.

Oxide heterointerfaces provide a wide range of emergent intriguing quantum phenomena inaccessible in their bulk individuals due to the strong interplay between electrons with Coulomb interaction and the interfacial electron-phonon coupling^{1–3}. Among them, a landmark oxide interface is the $\text{LaAlO}_3/\text{SrTiO}_3$ ⁴, which exhibits a plethora of appealing physical properties, including two-dimensional electron gases with high electron mobility⁵, strong Rashba-like spin-orbit coupling^{6–8}, interfacial superconductivity^{9,10}, and ferromagnetism^{11,12}. In particular, the coexistence of superconductivity and ferromagnetism has also been unravelled in the measurements of high-resolution magnetic torque magnetometry¹³, scanning superconducting quantum interference device¹⁴, and magnetoresistance¹⁵, indicative of a possible unconventional and nontrivial superconducting phase as the ground state, such as a candidate of intriguing Fulde-Ferrell-Larkin-Ovchinnikov-type condensate of Cooper pairs with finite momentum¹⁶ and a mixed-parity superconducting state with an admixture of spin-singlet and spin-triplet pairing components¹⁷. However, the extremely low superconducting critical temperature T_c (below 250 mK) of SrTiO_3 heterointerfaces is a critical challenge^{9,18,19}, leading to that the origin of these quantum states remains elusive^{20–22}.

Very recently, an unexpected crystalline-orientation-dependent superconductivity has been observed at the KTaO_3 heterointerfaces with T_c of 2 K^{23,24}, showing near two orders of magnitude higher in T_c than its three-dimensional counterpart²⁵. These experimental findings also suggest that the electronic states near the Fermi level derived from Ta $5d$ orbitals with strong spin-orbit coupling play a decisive role in electronic conduction at the KTaO_3 heterointerfaces^{26–28}. Furthermore, the exis-

tence of intrinsic anomalous Hall effect observed in electrical transport measurements has been revealed at the non-superconducting KTaO_3 heterointerfaces²⁹, indicative of the emergent ferromagnetism with time-reversal symmetry breaking. In addition, at the superconducting KTaO_3 heterointerfaces, both the in-plane azimuthal angle-dependent magnetoresistance and superconducting critical field are found to exhibit striking twofold symmetric oscillations deep inside the superconducting phase that the anisotropy vanishes in the normal phase, suggestive of an intrinsic nature of the mixed-parity unconventional superconducting ground state with an admixture of s -wave and p -wave pairing components inherent to the inversion symmetry breaking at the KTaO_3 heterointerfaces³⁰. Theoretically, although the component of p -wave pairing could be stabilized by the long-range ferromagnetic order^{31–33}, the existence of ferromagnetism at the superconducting KTaO_3 heterointerfaces, similar to that observed at the superconducting SrTiO_3 heterointerfaces, has yet to be addressed experimentally.

Here, using the measurements of direct current superconducting quantum interference device, we observe the conspicuous signal of in-plane ferromagnetic hysteresis loop at the verge of two-dimensional superconductivity at the KTaO_3 heterointerfaces, assigning to intrinsic ferromagnetism that persists up to room temperature. Moreover, the first-principles calculations provide an additional evidence of the robust ferromagnetism for the intrinsic property of the KTaO_3 heterointerfaces that the local moments on the Ta⁴⁺: $5d^1$ ions brought about by the oxygen vacancies that host the two-dimensional electron gases formed at the KTaO_3 heterointerfaces. Therefore, these results indicate the KTaO_3 heterointerface to be the time-reversal symmetry breaking superconductor,

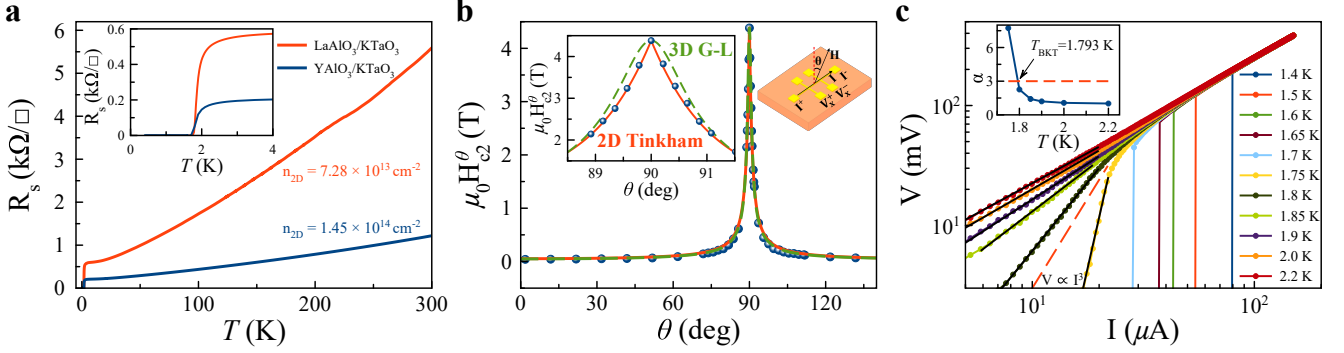


FIG. 1. **Two-dimensional superconductivity of KTaO₃ heterointerfaces.** **a**, Longitudinal electrical resistance R_s as a function of temperature for LaAlO₃ and YAlO₃ films grown on the KTaO₃(111) substrates. Inset: magnified view of low temperature regime. **b**, Out-of-plane polar angular θ dependence of the upper critical field $\mu_0 H_{c2}^\theta$ for LaAlO₃/KTaO₃(111). Inset: magnified view of the regime around $\theta = 90^\circ$. The red solid line and green dotted line are the theoretical fitting results using the two-dimensional (2D) Tinkham and the three-dimensional (3D) anisotropic Ginzburg-Landau (G-L) models, respectively. **c**, I-V measurements at various temperatures on logarithmic scale for LaAlO₃/KTaO₃(111). The red dashed line represents $V \propto I^3$. Inset: the extracted power-law fitting exponent α as a function of the temperature T . The BKT transition temperature $T_{\text{BKT}} = 1.793$ K is defined by $\alpha = 3$.

which brings a new broad of perspective on understanding the underlying rich superconducting properties at the KTaO₃ heterointerfaces.

Experimental results.—Both the LaAlO₃ and YAlO₃ thin films are grown by pulsed laser deposition on top of the $5 \times 5 \times 0.5$ mm³ single-crystalline KTaO₃(111) substrates (see Methods and our previous study³⁰). Atomic force microscopy characterization shows that the surface of KTaO₃ substrates and thin films are atomically flat (see Supplementary Fig. 1, YAlO₃ shown in Ref. 30), suggesting high-quality growth of the thin films on KTaO₃. Whereas the absence of epitaxial Bragg reflection peaks from both the LaAlO₃ and YAlO₃ thin films is revealed by X-ray diffraction (see Supplementary Fig. 2, YAlO₃ shown in Ref. 30), demonstrating that the amorphous phase of both the LaAlO₃ and YAlO₃ thin films is deposited on the KTaO₃(111) substrates. These results are in good agreement with the previous studies^{23,24,30,34}. In the followings, the electrical transport measurements are performed on the as-grown thin films patterned Hall bar configurations^{30,35}.

The longitudinal electrical resistances R_s in Fig. 1a shows metallic behavior from room temperature to 2.5 K for both the heterostructures of LaAlO₃/KTaO₃(111) and YAlO₃/KTaO₃(111), indicating that the two-dimensional electron gases are formed at their heterointerfaces since the bulks of LaAlO₃, YAlO₃, and KTaO₃ are nonmagnetic insulators. In addition, the charge carriers in both the LaAlO₃/KTaO₃(111) and YAlO₃/KTaO₃(111) are revealed to be electrons with the estimated charge carrier density of 7.28×10^{13} cm⁻² and 1.45×10^{14} cm⁻², respectively. Notably, the superconducting transitions start at $T_c^{\text{onset}} = 2.32$ K and 2.39 K, and resistances drop to zero at $T_c^{\text{zero}} = 1.66$ K and 1.7 K, respectively, for LaAlO₃/KTaO₃ and YAlO₃/KTaO₃. At the superconducting heterointerface of LaAlO₃/KTaO₃(111), the field-dependent resistance

shown in Supplementary Fig. 3 yields the upper critical fields $\mu_0 H_{c2}^\parallel(0.6 \text{ K}) = 5$ T for fields parallel to the sample plane surface and $\mu_0 H_{c2}^\perp(0.6 \text{ K}) = 0.45$ T for fields parallel to the crystallographic c -axis. Here, the $\mu_0 H_{c2}$ is defined as the magnetic field at the midpoint of the electrical resistance transition. The extracted temperature dependence of the upper critical fields $\mu_0 H_{c2}$ is shown in Supplementary Fig. 3c, and we find the existence of large ratio of $H_{c2}^\parallel/H_{c2}^\perp$, which suggests the strong anisotropic superconductivity of LaAlO₃/KTaO₃(111). Quantitatively, the out-of-plane polar angular θ -dependent upper critical field $\mu_0 H_{c2}^\theta$ at 1.6 K is used to further verify this intriguing behavior, as shown in Fig. 1b. Using the two-dimensional Tinkham and the three-dimensional anisotropic Ginzburg-Landau models to fit the $\mu_0 H_{c2}^\theta$, given by $\frac{H_{c2}^\theta |\cos \theta|}{H_{c2}^\perp} + \left(\frac{H_{c2}^\theta \sin \theta}{H_{c2}^\parallel}\right)^2 = 1$ and $\left(\frac{H_{c2}^\theta \cos \theta}{H_{c2}^\perp}\right)^2 + \left(\frac{H_{c2}^\theta \sin \theta}{H_{c2}^\parallel}\right)^2 = 1$, respectively^{36,37}, a cusp-like peak is clearly observed at around $\theta = 90^\circ$ (see Fig. 1b, inset), which is well described by the two-dimensional Tinkham model, as frequently observed in heterointerface superconductivity^{30,37,38} and layered transition metal dichalcogenides^{31,39}. Qualitatively similar results have also been observed in YAlO₃/KTaO₃³⁰, unambiguously demonstrating the intrinsic two-dimensional superconductivity at the KTaO₃ heterointerfaces.

To further examine the intrinsic interfacial superconductivity at the KTaO₃ heterointerfaces, we also measure the current-voltage (I-V) characteristics at various temperatures close to T_c (see Supplementary Fig. 4) and show using log-log scale in Fig. 1c. Below T_c , we find a clear critical current I_c of 79.1 μA at a temperature of 1.4 K. With increasing temperature, the value of critical current I_c gradually decreases to zero, signaling a transition from superconducting to metallic states. In the normal state, the relationship between voltage and current is expressed as $V \propto I$ that is Ohm's law. As temperature

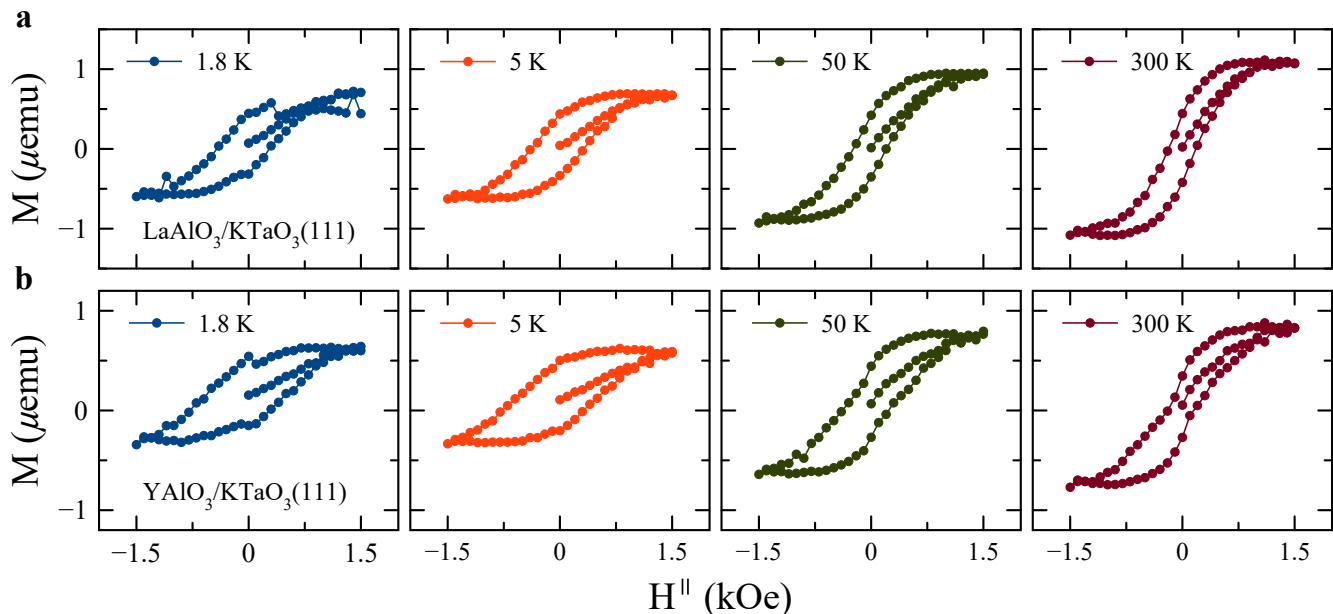


FIG. 2. **Ferromagnetic properties of KTaO₃ heterointerfaces.** Temperature-dependent in-plane M - H^{\parallel} ferromagnetic hysteresis loops of **a**, LaAlO₃/KTaO₃(111) and **b**, YAlO₃/KTaO₃(111) after the subtraction of the diamagnetic contribution of the bare KTaO₃ substrate at different temperatures. A magnetic field H^{\parallel} is applied parallel to the surface of thin films ranging from -1.5 kOe to +1.5 kOe.

drops, a steeper power law $V \propto I^{\alpha(T)}$ is smoothly evolved. Using the Berezinskii-Kosterlitz-Thouless (BKT) definition^{40,41}, the transition temperature T_{BKT} corresponds to the dissociation of vortex-antivortex pairs obeying the universal scaling relation $V \propto I^3$, since the superconducting phase consists of bound vortex-antivortex pairs in two-dimensional superconductors. We thus determine $T_{\text{BKT}} = 1.793$ K from where $\alpha = 3$ interpolates. Besides, the T_{BKT} can be alternatively evaluated from the formula $R_s = R_0 \exp[-b(T/T_{\text{BKT}} - 1)^{-1/2}]$, where R_0 and b are material parameters⁴². Application of such theoretical fit to the measured R_s yields $T_{\text{BKT}} = 1.878$ K (see Supplementary Fig. 5). As expected, the T_{BKT} obtained from these two independent approaches appears to be close to T_c^{zero} , providing the compelling evidence for the two-dimensional superconducting nature of the KTaO₃ heterointerfaces.

Next, we turn to discuss the magnetic properties at the KTaO₃ heterointerfaces, since the two-dimensional conducting electron gases formed at the interface of KTaO₃ heterostructures are primarily derived from the contribution of the partially filled $5d$ orbitals of the Ta atoms induced by oxygen vacancies that can lead to ferromagnetism (also see the first-principles calculations in details). The zero-field-cooling (ZFC) and field-cooling (FC) curves of the as-grown thin films of LaAlO₃ and YAlO₃ measured at temperature between 1.8 and 300 K with an applied in-plane field of 50 Oe are summarized in Supplementary Fig. 6. Remarkably, the figures clearly show that the separation between the ZFC and the FC curves obtained for the same magnetic field value occurs up to 300 K, implying the existence

of the in-plane ferromagnetism at the superconducting KTaO₃ heterointerfaces that persists to room temperature. Figure 2 shows the well-defined $M \sim H^{\parallel}$ hysteresis loops measured at different temperatures for the heterostructures of LaAlO₃/KTaO₃ and YAlO₃/KTaO₃, unambiguously demonstrating that the temperature dependence of long-range ferromagnetic order appears and lies in-plane of the KTaO₃ heterointerfaces. Here, it should be noted that there is an overlapping ferromagnetic response in addition to the diamagnetic or paramagnetic response, as seen in the form of in-plane hysteresis loop extending up to room temperature (Supplementary Fig. 7 and Supplementary Fig. 8, also shown in Fig. 2 after background subtraction), since the standard temperature-independent diamagnetic contribution of the KTaO₃ substrates is discernible during these field sweep curves (Supplementary Fig. 9). Such an in-plane ferromagnetism in the nonmagnetic LaAlO₃/KTaO₃ and YAlO₃/KTaO₃ is surprising due to the absence of intrinsically magnetic component in our samples, indicating that KTaO₃ is the primary source of this interfacial magnetism, which is essentially different from previous report that is thought to be derived from magnetic thin film EuO⁴³. Furthermore, comparing with the absence of ferromagnetic hysteresis loop in the as-received KTaO₃ substrates (Supplementary Fig. 9), the observed magnetic signal is probably related to Ta⁴⁺ : $5d^1$ that is induced by the high concentration oxygen vacancies at the KTaO₃ heterointerfaces. We thus evaluate the in-plane magnetization of the itinerant electron gases formed at the KTaO₃ heterointerfaces with magnitude corresponding to $\simeq 0.2 \mu_B$ per interface unit cell (if all the magnetization

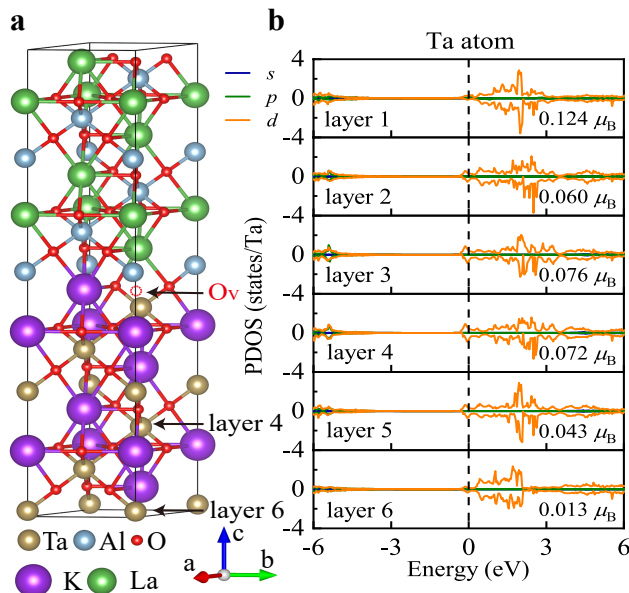


FIG. 3. First-principles calculations on the KTaO₃ heterointerface. **a**, Schematic structure of the superlattices (LaAlO₃)₆/(KTaO₃)₆(111) with the presence of an oxygen vacancy for the theoretical simulations. Here, the red dotted circle marks the oxygen vacancy (O_v) at the heterointerface of LaAlO₃/KTaO₃(111). **b**, The calculated PDOS for Ta atoms by using GGA+ U_{eff} method with $U_{\text{eff}} = 1.0$ eV. Here, the numbers listed in the figure represent the magnetization of Ta in each layer.

is assigned to the interface). Notably, at the lowest temperature of this measurement limited $T = 1.8$ K, which is also lower than T_c^{onset} [2.32 K for LaAlO₃/KTaO₃(111) and 2.39 K for YAlO₃/KTaO₃(111)], the conspicuous signal of in-plane ferromagnetic hysteresis loops is observed in the superconducting transition regime and the magnetization does not seem to be expelled below T_c . This striking result is strong reminiscent of the intrinsic spatial coexistence of superconductivity and long-range ferromagnetic order at the KTaO₃ heterointerfaces⁴⁴.

To gain further insight into the emergent intrinsic ferromagnetism at the KTaO₃ heterointerfaces, we proceed to discuss the underlying electronic and magnetic properties based on the first-principles calculations^{45–47}. For simplicity, we construct a theoretical model with the superlattice (KTaO₃)₆/(LaAlO₃)₆(111) containing the supercell of six layers of both the LaAlO₃ and KTaO₃ for simulating the interfacial electronic states⁴⁸, albeit the amorphous phase of LaAlO₃ thin films grown on the KTaO₃(111) substrates (see Supplementary Fig. 2), as schematically illustrated in Fig. 3a and Supplementary Fig. 10a (also see Methods). In the stoichiometric heterostructure of (KTaO₃)₆/(LaAlO₃)₆(111) that is absence of oxygen vacancy, the calculated layer-dependent projected density-of-states (PDOS) reveal the system to be a nonmagnetic band insulator with an energy band gap of ≈ 3.0 eV, in good agreement with previous study⁴⁹. Interestingly, this result also indicates that the diverging

Coulomb field due to the polarity of the individual layers of LaAlO₃ and KTaO₃ is unlikely to be the source of the emergent two-dimension electron gases formed at the KTaO₃ heterointerfaces, instead by the existence of oxygen vacancies.

Since each oxygen vacancy, in principle, donates two electrons into the LaAlO₃/KTaO₃(111) interface, the induced interface charges are typically spread over adjacent layers, giving rise to a Ta⁴⁺~O²⁻~Ta⁵⁺-like electronic configuration, which corresponds to several partially filled Ta 5d sub-bands that can lead to interfacial ferromagnetism. As expected, density functional theory calculations show that in the presence of oxygen vacancies (O_v, marked by red dotted circle shown in Fig. 3a), the system behaves a metal with the conducting electrons mainly derived from the Ta 5d orbitals partially hybridized with the oxygen 2p orbitals (see Supplementary Fig. 11). Furthermore, Fig. 3b shows the spin-resolved PDOS for Ta atoms associated with the value of its magnetic moments of each Ta layer. The calculated magnetic moment of Ta brought about by the nearby oxygen vacancy is about 0.124 μ_B, indicating that the long-range ferromagnetic order is an intrinsic property of the KTaO₃ heterointerface. These theoretical calculated results are in both qualitative and quantitative agreement with the magnetization measurements shown in Fig. 2. Here, it should be worthy pointing out that the electron correlation effect of Ta 5d orbitals has been corrected via the simplified on-site repulsion strength U_{eff} on Ta 5d orbitals⁵⁰, which reproduces the magnetic moment that is fairly consistent with the experimental findings (Supplementary Fig. 12).

In summary, we have experimentally grown two-dimensional superconducting heterointerfaces of the KTaO₃ and observed striking in-plane ferromagnetic hysteresis loops at the verge of superconductivity that persists up to room temperature. In addition, the first-principles calculations are also carried out to further elucidate the intrinsic ferromagnetism emergent at the heterointerfaces of the KTaO₃. These intriguing findings indicate the KTaO₃ heterointerfaces to be an unconventional superconductivity with time-reversal symmetry breaking, which has long been a topic of interest sought in condensed matter physics and material science, and will stimulate a great deal of both experimental and theoretical studies to further unveil the delicate interplay among the strong spin-orbit coupling, ferromagnetism, and superconductivity at the newly discovered KTaO₃ heterointerfaces.

Acknowledgements

This work is supported by the National Natural Science Foundation of China (Grant No. 11927807) and Shanghai Science and Technology Committee (Grant No. 20DZ1100604).

Author contributions

Z.N., J.Q., and Y.L. contributed equally to this work.

W.L. conceived the project and designed the experiments. Z.N. and G.Z. grew the samples. Z.N., Y.L., F.C., G.Z., and G.M. performed the electrical transport measurements. Z.N. and Y.L. performed the magnetization measurements. J.Q. performed the first-principles calculations. W.L. wrote the paper with input from Z.N. and J.Q.. All authors discussed the results and gave approval to the final version of the manuscript.

Competing interests

The authors declare no competing interests.

Additional information

Supplementary information

Data availability

The relevant data supporting our key findings are available within the article and the Supplementary Information file. All raw data generated during our current study are available from the corresponding authors upon reasonable request.

Correspondence and requests for materials should be addressed to G. Mu or W. Li.

*To whom correspondence should be addressed. E-mail: mugang@mail.sim.ac.cn or w.li@fudan.edu.cn

-
- ¹ Mannhart, J. & Schlom, D. G. Oxide interfaces—an opportunity for electronics. *Science* **327**, 1607-1611 (2010).
 - ² Zubko, P. et al. Interface physics in complex oxide heterostructures. *Annu. Rev. Condens. Matter Phys.* **2**, 141-165 (2011).
 - ³ Hwang, H. Y. et al. Emergent phenomena at oxide interfaces. *Nat. Mater.* **11**, 103-113 (2012).
 - ⁴ Huijben, M. et al. Structure-property relation of SrTiO₃/LaAlO₃ interfaces. *Adv. Mater.* **21**, 1665-1677 (2009).
 - ⁵ Ohtomo, A. & Hwang, H. Y. A high-mobility electron gas at the LaAlO₃/SrTiO₃ heterointerface. *Nature* **427**, 423-426 (2004).
 - ⁶ Shalom, M. B. et al. Tuning spin-orbit coupling and superconductivity at the SrTiO₃/LaAlO₃ interface: A magnetotransport study. *Phys. Rev. Lett.* **104**, 126802 (2010).
 - ⁷ Caviglia, A. et al. Tunable Rashba Spin-Orbit Interaction at Oxide Interfaces. *Phys. Rev. Lett.* **104**, 126803 (2010).
 - ⁸ Soumyanarayanan, A. et al. Emergent phenomena induced by spin-orbit coupling at surfaces and interfaces. *Nature* **539**, 509-517 (2016).
 - ⁹ Reyren, N. et al. Superconducting interfaces between insulating oxides. *Science* **317**, 1196-1199 (2007).
 - ¹⁰ Caviglia, A. D. et al. Electric field control of the LaAlO₃/SrTiO₃ interface ground state. *Nature* **456**, 624-627 (2008).
 - ¹¹ Brinkman, A. et al. Magnetic effects at the interface between non-magnetic oxides. *Nat. Mater.* **6**, 493-496 (2007).
 - ¹² Ariando. et al. Electronic phase separation at the LaAlO₃/SrTiO₃ interface. *Nat. Commun.* **2**, 188 (2011).
 - ¹³ Li, L. et al. Coexistence of magnetic order and two-dimensional superconductivity at LaAlO₃/SrTiO₃ interfaces. *Nat. Phys.* **7**, 762-766 (2011).
 - ¹⁴ Bert, J. A. et al. Direct imaging of the coexistence of ferromagnetism and superconductivity at the LaAlO₃/SrTiO₃ interface. *Nat. Phys.* **7**, 767-771 (2011).
 - ¹⁵ Dikin, D. et al. Coexistence of superconductivity and ferromagnetism in two dimensions. *Phys. Rev. Lett.* **107**, 056802 (2011).
 - ¹⁶ Michaeli, K., Potter, A. C. & Lee, P. A. Superconducting and ferromagnetic phases in SrTiO₃/LaAlO₃ oxide interface structures: Possibility of finite momentum pairing. *Phys. Rev. Lett.* **108**, 117003 (2012).
 - ¹⁷ Kozii, V. & Fu, L. Odd-parity superconductivity in the vicinity of inversion symmetry breaking in spin-orbit-coupled systems. *Phys. Rev. Lett.* **115**, 207002 (2015).
 - ¹⁸ Han, Y.-L. et al. Two-dimensional superconductivity at (110) LaAlO₃/SrTiO₃ interfaces. *Appl. Phys. Lett.* **105**, 192603 (2014).
 - ¹⁹ Monteiro, A. et al. Two-dimensional superconductivity at the (111)LaAlO₃/SrTiO₃ interface. *Phys. Rev. B* **96**, 020504(R) (2017).
 - ²⁰ Fitzsimmons, M. R. et al. Upper limit to magnetism in LaAlO₃/SrTiO₃ heterostructures. *Phys. Rev. Lett.* **107**, 217201 (2011).
 - ²¹ Salman, Z. et al. Nature of weak magnetism in SrTiO₃/LaAlO₃ multilayers. *Phys. Rev. Lett.* **109**, 257207 (2012).
 - ²² Pai, Y.-Y., Tylan-Tyler, A., Irvin, P. & Levy, J. *Spintronics Handbook: Spin Transport and Magnetism*. (CRC Press, 2019).
 - ²³ Liu, C. et al. Two-dimensional superconductivity and anisotropic transport at KTaO₃ (111) interfaces. *Science* **371**, 716-721 (2021).
 - ²⁴ Chen, Z. et al. Two-dimensional superconductivity at the LaAlO₃/KTaO₃(110) heterointerface. *Phys. Rev. Lett.* **126**, 026802 (2021).
 - ²⁵ Ueno, K. Discovery of superconductivity in KTaO₃ by electrostatic carrier doping. *Nat. Nanotechnol.* **6**, 408-412 (2011).
 - ²⁶ Bruno, F. Y. et al. Band structure and spin-orbital texture of the (111)-KTaO₃ 2D electron gas. *Adv. Electron. Mater.* **5**, 1800860 (2019).
 - ²⁷ Mallik, S. et al. Superfluid stiffness of a KTaO₃-based two-dimensional electron gas. *Nat. Commun.* **13**, 4625 (2022).
 - ²⁸ Hua, X. et al. Tunable two-dimensional superconductivity and spin-orbit coupling at the EuO/KTaO₃(110) interface. *npj Quantum Mater.* **7**, 97 (2022).
 - ²⁹ Krantz, P. et al. Emergent magnetism and intrinsic anomalous Hall effect in KTaO₃ two-dimensional electron gases. arXiv:2209.10534 (2022).
 - ³⁰ Zhang, G. et al. Spontaneous rotational symmetry breaking in KTaO₃ interface superconductor. arXiv:2111.05650 (2021).
 - ³¹ Jiang, D. et al. Strong in-plane magnetic field induced reemergent superconductivity in the van der Waals heterointerface of NbSe₂ and CrCl₃. *ACS Appl. Mater. Interfaces* **12**, 49252-49257 (2020).

- ³² Zou, M. et al. Evidence for ferromagnetic order in the CoSb layer of LaCoSb₂. *Phys. Rev. B* **101**, 155138 (2020).
- ³³ Yuan, T.-Z. et al. Pairing symmetry in monolayer of orthorhombic CoSb. *Front. Phys.* **16**, 43500 (2021).
- ³⁴ Chen, Z. et al. Electric field control of superconductivity at the LaAlO₃/KTaO₃(111) interface. *Science* **372**, 721-724 (2021).
- ³⁵ Xue, H. et al. Fourfold symmetric superconductivity in spinel oxide LiTi₂O₄(001) thin films. *ACS Nano* **16**, 19464-19471 (2022).
- ³⁶ Tinkham, M. Effect of fluxoid quantization on transitions of superconducting films. *Phys. Rev.* **129**, 2413-2422 (1963).
- ³⁷ Wang, L. et al. Two-dimensional superconductivity at the titanium sesquioxide heterointerface. *ACS Nano* **16**, 16150-16157 (2022).
- ³⁸ Zhang, G. et al. Quantum metallic state in the titanium sesquioxide heterointerface superconductor. arXiv:2211.04035 (2022).
- ³⁹ Lu, J. M. et al. Evidence for two-dimensional Ising superconductivity in gated MoS₂. *Science* **350**, 1353-1357 (2015).
- ⁴⁰ Kosterlitz, J. M. & Thouless, D. J. Long range order and metastability in two dimensional solids and superfluids. *J. Phys.: Condens. Matter* **5**, L124-L126 (1972).
- ⁴¹ Beasley, M. R., Mooij, J. E. & Orlando, T. P. Possibility of vortex-antivortex pair dissociation in two-dimensional superconductors. *Phys. Rev. Lett.* **42**, 1165-1168 (1979).
- ⁴² Halperin, B. I. & Nelson, D. R. Resistive transition in superconducting films. *J. Low Temp. Phys.* **36**, 599-616 (1979).
- ⁴³ Zhang, H. et al. High-mobility spin-polarized two-dimensional electron gases at EuO/KTaO₃ interfaces. *Phys. Rev. Lett.* **121**, 116803 (2018).
- ⁴⁴ Pfeleiderer, C. Superconducting phases of *f*-electron compounds. *Rev. Mod. Phys.* **81**, 1551-1624 (2009).
- ⁴⁵ Zhou, Z. et al. Universal critical behavior in the ferromagnetic superconductor Eu(Fe_{0.75}Ru_{0.25})₂As₂. *Phys. Rev. B* **100**, 060406(R) (2019).
- ⁴⁶ Huang, W.-C., Li, W. & Liu, X. Exotic ferromagnetism in the two-dimensional quantum material C₃N. *Front. Phys.* **13**, 137104 (2018).
- ⁴⁷ Li, W. et al. First-principles calculations of the electronic structure of iron-pnictide EuFe₂(As,P)₂ superconductors: Evidence for antiferromagnetic spin order. *Phys. Rev. B* **86**, 155119 (2012).
- ⁴⁸ Popović, Z. S., Satpathy, S. & Martin, R. M. Origin of the two-dimensional electron gas carrier density at the LaAlO₃ on SrTiO₃ interface. *Phys. Rev. Lett.* **101**, 256801 (2008).
- ⁴⁹ Fujii, Y. & Sakudo, T. Dielectric and optical properties of KTaO₃. *J. Phys. Soc. Jpn.* **41**, 888-893 (1976).
- ⁵⁰ Pentcheva, R. & Pickett, W. E. Correlation-driven charge order at the interface between a Mott and a band insulator. *Phys. Rev. Lett.* **99**, 016802 (2007).